Lasers Med Sci (2017) 32:1545–1560
DOI 10.1007/s10103-017-2278-7

ORIGINAL ARTICLE

Evaluation of the effects of photobiomodulation on vertebras in two rat models of experimental osteoporosis

Mohammadjavad Fredoni[1] · Mahdi Ghatrehsamani[2] · Mohammad-amin Abdollahifar[3] · Sahar Bayat[4] · Mohammad Bayat[5]

Received: 15 July 2016 / Accepted: 29 June 2017 / Published online: 19 July 2017

Abstract The aim of this study was to evaluate the effects of photobiomodulation (PBM) on cancellous bone in rat models of ovariectomized induced osteoporosis (OVX-D) and glucocorticoid-induced osteoporosis (GIOP). The experiment comprised of nine groups. A group of healthy rats was used for baseline evaluations. The OVX-D rats were further divided into groups as follows: control rats with osteoporosis, OVX-D rats that received alendronate (1 mg/kg 60 days), OVX-D rats treated with pulsed wave laser (890 nm, 80 Hz, 900 s, 0.0061 W/cm^2, 5.5 J/cm^2, three times a week, 60 days), and OVX-D rats treated with alendronate + pulsed laser. Dexamethasone was administered to the remaining rats that were split into four groups: control, alendronate-treated rats, laser-treated rats, and GIOP rats treated with alendronate + laser. T12, L1, L2, and L3 vertebrae were subjected to laser. Results of the current study demonstrated that OVX-D and GIOP significantly decreased some stereological parameters, and type 1 collagen gene expression compared to the healthy group. There was a significant increase in osteoclast number in both OVX-D and glucocorticoid administration compared to the healthy group. However, the detrimental effect of the OVX-D procedure on bone was more serious than glucocorticoid administration. Results showed that laser alone had a detrimental effect on trabecular bone volume, and cortical bone volume in groups GIOP and OVX-D compared to those in the healthy group. Alendronate significantly improved total vertebral bone volume, trabecular bone volume, and cortical bone volume, in GIOP and OVX-D groups compared to the laser-treated groups. Furthermore, the alendronate + laser in OVX-D rats and GIOP rats produced significantly increased osteoblast number and type 1 collagen gene expression and caused a significant decrease in osteoclast number compared to the controls.

Keywords Osteoporosis · Photobiomodulation · Low-level laser therapy · Glucocorticoid-induced osteoporosis · Ovariectomized induced osteoporosis · Vertebra · Stereology · Real-time polymerase chain reaction · Rat

✉ Mohammad Bayat
mohbayat@sbmu.ac.ir; bayat_m@yahoo.com

Mohammadjavad Fredoni
fredoni_javad@yahoo.com

Mahdi Ghatrehsamani
mahdi.samani.2020@gmail.com

Mohammad-amin Abdollahifar
m_amin58@yahoo.com

Sahar Bayat
aharnazbt@yahoo.com

[1] Department of Anatomy, School of Medicine, Zanjan University of Medical Sciences, Zanjan, Iran

[2] Cellular and Molecular Biology Research Center, Shahrekord University of Medical Sciences, Shahrekord, Iran

[3] Department of Biology and Anatomical Sciences, School of Medicine, Shahid Beheshti University of Medical Sciences, Tehran, Iran

[4] No. 1 Farzanegan High School, Tehran, Iran

[5] Cellular and Molecular Biology Research Center, Department of Anatomical Sciences and Biology, School of Medicine, Shahid Beheshti University of Medical Sciences, 19395/4719, Tehran 1985717443, Iran

Abbreviations

OP	Osteoporosis
GC	Glucocorticoid
GIOP	Glucocorticoid (GC)-induced OP
ECM	Extracellular matrix
TGF-β	Transforming growth factor beta
IGF-I	Insulin-like growth factor-I
BMPs	Bone morphogenetic proteins
rhPTH	Recombinant human parathyroid hormone
PBM	Photobiomodulation
PW	Pulse wave
ALP	Alkaline phosphatase
LED	Light-emitting diode
RANKL	Receptor activator of nuclear factor kappa-B ligand
CW	Continuous wave
OPG	Osteoprotegerin
GaAlAs	Gallium aluminum arsenide
OVX-D	Ovariectomized induced OP
RT-PCR	Real-time polymerase chain reaction
H	Healthy
H&E	Hematoxylin and eosin
ANOVA	One-way analysis of variance
BMD	Bone mineral density
DXA	Dual-energy X-ray absorptiometry
GTP	Guanosine triphosphate
PPARγ	Peroxisome proliferator-activated receptor-γ
RUNX	Runt-related transcription factor

Introduction

Bone tissue formation, maintenance, and repair depend on finely tuned interaction of osteoclasts and osteoblasts. Bone tissue is in a constant process of remodeling that involves regeneration of its matrix; osteoblasts have a role in new bone matrix deposits, while osteoclasts are involved in degrading the old matrices. In a postmenopausal skeleton, regenerative bone formation in the arm ultimately declines, the process is known as primary osteoporosis (OP) [1]. Glucocorticoid (GC)-induced OP (GIOP) is the most common cause of secondary OP [2]. OP is a skeletal disorder distinguished by low bone mass and micro-architectural deterioration of the bone tissue that makes bones vulnerable and susceptible to fracture [3]. Estimates show that among adults aged 50 years and over in the USA (2010), 10.3% or 10.2 million people suffered from OP in some region of the body such as in the femoral neck or the lumbar spine [4]. OP can lead to fracture even in cases of mild trauma, so it is very important to maintain and treat patients with osteoporosis in order to prevent fracture [5]. Osteoporotic fracture has become a common condition but no satisfactory treatment has been developed to date [6].

There are many cytokines and growth factors that govern bone cell activity during normal bone remodeling. The extracellular matrix (ECM) releases substances such as transforming growth factor beta (TGF-β) and insulin-like growth factor-I (IGF-I) during bone resorption. These factors recruit and activate osteoblasts to begin collagen synthesis. Collagen type 1 is involved in skeletal development and has a regulatory effect on bone cells [7]. The process of osteoblast maturation is affected by activity of various endocrine, paracrine, and autocrine processes. These factors include a number of bone morphogenetic proteins (BMPs) and IGF-I. The recombinant human BMP-2 is a medical administration used to facilitate spinal fusion and is approved for OP therapy [8].

Prevention of OP and its complications is an essential socioeconomic priority [9].

Drug agents for the treatment of OP are defined as either antiresorptive (catabolic) or anabolic. Antiresorptive agents such as bisphosphonate work by reducing osteoclast activity and thus declining bone resorption. Teriparatide (recombinant human parathyroid hormone $(rPTH)_{1–34}$) is the only anabolic agent currently available in the USA. PTH stimulates osteoblast function and bone formation of vertebral fracture [10]. Treatment with anabolic agents such as photobiomodulation (PBM) is a strong stimulant for bone turnover and seems to be a superior treatment compared with alendronate [11]. Some investigations have demonstrated that laser irradiation had a positive effect on osteoblasts in vitro. Ueda and Shimizu reported that pulsed wave (PW) laser significantly stimulated cellular proliferation, bone nodule formation, alkaline phosphatase (ALP) activity, and ALP gene expression, compared with a non-irradiation group [12, 13]. Sohn et al. report on an investigation on the impact of 635-nm irradiation dose from a light-emitting diode (LED) on osteoclastogenesis in vitro. It was reported that LED irradiation significantly inhibited receptor activator of nuclear factor kappa-B ligand (RANKL)-mediated osteoclast differentiation from bone marrow-derived macrophages. Sohn et al. present LED irradiation/laser as an alternative, conservative approach to OP management [14]. Kiyosaki et al. reported the effects of continuous wave (CW) laser on osteoblasts via insulin-like growth factor I (IGF-I) signal transduction. The report suggests that laser escalates in vitro mineralization by increasing IGF-I and BMP production [15]. Xu et al. reported on the effect of laser (650 nm, 2 mW, 2.28 J/cm^2, 6000 Hz) on messenger RNA (mRNA) expression of RANKL and osteoprotegerin (OPG) in rat calvarial cells. Xu et al. suggested that laser may have promoted osteoblast proliferation and differentiation directly, and indirectly inhibited of osteoclast differentiation by downregulating the RANKL:OPG mRNA ratio in osteoblasts. Thus, other research has shown that laser was beneficial for treating

bone diseases such as OP [16]. In vivo studies have suggested that both CW laser (632.8 nm, 10 mW, 382.2 J/cm^2) and laser (890 nm, 80 Hz, 0.972 J/cm^2) improved biomechanical properties of tibia and vertebra compared to healthy bones in rats [17–19]. Consistent with other reports, it has been confirmed that laser (830-nm gallium aluminum arsenide (GaAlAs) laser diode, 5 and 15 J/cm^2) not only made changes in thickness of the epiphyseal cartilage but also increased the number of the chondrocytes [20].

However, research has some controversy over the benefits of PBM for treatment of OP. Several studies have reported a positive effect of PBM on ovariectomized induced OP (OVX-D) rats, and orthodontic tooth movement on post-menopausal women [21–24], whereas others have reported no improvement in OVX-D and GIOP OP models subjected to PBM [25–30]. To the best of our knowledge, no study has yet examined the effects of laser on gene expression and stereological analyses of histological parameters in the vertebrae of OVX-D and GIOP rats. Paraclinical information such as bone mineral density (BMD), biochemical markers, histological parameters, and gene expression findings can assist clinicians in determining treatment for patients with OP [31]. The aim of this study was to assess the effects of PBM on trabecular bone in two rat models of OP. A stereological analysis of histological parameters was done to make determinations for total volume of vertebral bone, cortical bone volume, trabecular bone volume, and total bone marrow volume and by evaluating numbers of osteocyte, osteoblast, and osteoclast. TGF-β, IGF-I, BMP-2, and type 1 collagen gene expressions were measured using the real-time polymerase chain reaction (RT-PCR) method.

Materials and methods

Animals and study design

Fifty-four adult male and female Wistar rats, aged 18 weeks, were housed in standard rat cages in a 12-h light/dark environment. Rats received water ad libitum. The procedure was approved by the Medical Ethics Committee of Shahid Beheshti University of Medical Sciences, Tehran, Iran (protocol no. 1391-1-115-1092). Rat body weight was measured weekly, and volumes of drug application were calculated according to the most recent body weight.

In this study, second and third vertebrae (L2 and L3) of both OVX-D and GIOP rats received pulsed laser and alendronate. L2 and L3 subsequently underwent a stereological analysis of histological parameters and RT PCR gene expression evaluation methods, respectively. The healthy (H) group (group 5) comprised six normal rats used as the baseline.

Sampling of OVX-D and GIOP groups

Fourty-eight rats were randomly divided into eight groups (six rats per group) and treated as follows: there were four groups of OVX-D rats and four groups of dexamethasone. OVX was made on rats under sterile conditions via two paravertebral skin incisions while rats were under general anesthesia. Uterine tubes were ligated, and incisions were closed after ovary removal. Rats received antibiotic therapy with ceftriaxone (50 mg/kg) immediately before and 24 and 48 h after surgery [26]. All animals were kept in cages for 14 weeks after surgery to allow development of OP [26]. At the end of this period, rats were subjected to the following treatments: group 1 (OC) comprised control rats with OP, group 2 (OA) were OVX-D rats treated subcutaneously with 1 mg/kg alendronate (Alborz Darou Co., Tehran, Iran), group 3 (OL) consisted of OVX-D rats that received laser three times weekly (Table 1), and group 4 (OAL) were OVX-D rats treated with laser and concomitant administration of alendronate (1 mg/kg). The remaining rats received a daily intramuscular (i.m.) dose of dexamethasone (1 mg/kg; Alborz Darou Co., Tehran, Iran), administered 6 days per week for 5 weeks [26]. After 5 weeks, dexamethasone-treated rats were subdivided into four groups: group 6 (control) consisted of OP rats treated with i.m. injection of vehicle (distilled water (DC)), group 7 (DA) or GIOP rats received alendronate, group 8 (DL) consisted of GIOP rats treated with laser (Table 1), and group 9 (DAL) was made up of GIOP rats treated with laser and alendronate.

Laser and alendronate administration

Hashmi et al., in their review article, reported that PW laser may be superior to CW light [32]. We observed the beneficial effects of the current PW laser protocol in previous studies [18, 19]. In these studies, PW laser had a remarkable effect on bone tissue at lower energy density compared to that of CW laser. A gallium–arsenide (GaAs) laser (Mustang 2000; Technical Co., Moscow, Russia) was used. All the laser radiation information were calculated and measured and shown in Table 2. Below, power density calculation was reported. T12, L1, L2, and L3 vertebrae were subjected to laser, three times per week for 2 months. The probe was fixed vertically with a portable holder at a distance of 0.5 cm above the skin (vertebras). Subcutaneous injections of alendronate at a dose of 1 mg/kg (Alborz Darou Co., Tehran, Iran) [26] were performed daily for 30 days.

Table 1 Specifications of the laser used

Parameters	Dose and unit
Peak power output at surface of probe and distance of 0.5 cm	69 and 59.5 W
Average power	0.001 mW
Power density	0.001 W/cm^2
Wavelength	890 nm
Pulse frequency	80 Hz
Spot shape and size of laser beam at the source	Oval, 0.05 cm^2
Spot shape and size of laser beam at distance of 0.5 cm	Oval, 0.14 cm^2
Pulsed duration	180 ns
Duration of exposure for each point	900 s
Energy densities at the surface of probe and at distance of 0.5	17.8 and 5.5 J/cm^2
Divergence angle: horizontal × vertical angle	25 × 10°
The frequency of treatment	Three times per week
Number of shootings per session	4
The cumulative dose (ED) given in each session	4 × 5.5 = 22 J/cm^2
The cumulative dose (ED) given totally (23 sessions)	23 × 22 = 506 J/cm^2

Light source and method of power density determination

$$Power\ density = energy\ density/duration\ of\ exposure \quad \text{for } each\ point$$
$$Power\ density = 5.5/900$$
$$Power\ density = 0.0061\ \mathrm{W/cm^2}$$

In the laser-treated groups, T12, L1, L2, and L3 vertebras were radiated with the laser probe that was held vertically to the bone at the distance of less than 10 mm for 2 months. During PW laser, animals were sedated by administration of 1/2 of the anesthetic drug dose. Rats received daily 30 mg/kg alendronate for 30 days. At 2 months, after the beginning of the treatment, all rats were euthanized by administration of an overdose of anesthesia. The L2 and L3 vertebrae were extracted carefully. L2 vertebral body used for histological examination and the L3 were frozen at −80 °C for RT-PCR gene expression analysis.

Histological and stereological examinations

The bones were fixed in formalin saline and decalcified in EDTA for 56 days. Primary volume *V* (primary) of vertebrae was measured using the immersion method [25]. Then, vertebrae were embedded in paraffin blocks and cut vertically into 5- and 25-μm-thick sections with a microtome. Slides were stained using hematoxylin and eosin (H&E) dye for microscopic descriptive analysis of each group. All measurements were taken using a magnifying objective (×4, ×40).

Stereological study

Measurement of bone volumes

Live images of each section of vertebra were evaluated using a projecting microscope. Following this procedure, eight to ten sections were obtained and analyzed for each vertebra. Volumes (*V*) were calculated using the Cavalieri method.

Table 2 Primers of the selected genes for quantitative real-time PCR

Gene	Gene ID	Primer sequences
TGF-beta1	NM_021578.2	Forward 5′ TAGCAACAATTCCTGGCGTTAC
		Reverse 5′ CCTGTATTCCGTCTCCTTGGTTC
IGF-I	NM_001082478.1	Forward 5′ GGAACATAAGGCACGCTGAAC
		Reverse 5′TGAGGAAGCAGGTAGATGGTGA
BMP-2	NM_017178.1	Forward 5′ AGAAGCCAGGTGTCTCCAAGA
		Reverse 5′ CCACATCACTGAAGTCCACATACA
Type1 collagen	NM_053304.1	Forward 5′ GGAGCAGCAAGAGCAAGGAG
		Reverse 5′ ACAGCAGGCGTAGGAAGGTC

Stereological software was used for grid points superimposed on the images. The total vertebral volume of L2 was estimated by the following formula:

$$V(bone) = \Sigma p \times a/p \times t$$

where Σp is the total of points hitting a vertebral bone section, a/p is the area associated with each point, and t is the distance between the sampled sections [25].

Estimation of number of bone cells

The dissector method was used to estimate numerical density and total number of bone cells. Specimens were evaluated at ×40 magnification with high numerical aperture. The captured images were sent to the image analysis computer. The focus plane was set at the surface of each specimen. Then, a set of three unbiased measurement frames was superimposed on the live image. At the same time, the microcator measuring the optical distance through the specimen in the z axis was zeroed. By gently moving the focus down through the specimen, an approximately 0.5-mm-thin focal plane made objects come into focus and then disappear. Bone cells that fell in the permitted area of the measurement frame were counted as they came into focus until the microcator showed that the focal plane had traveled 10 μm through the specimen. Numerical density of cells was obtained by

$$Nv = \Sigma Q^{-}/(h \times a/f \times \Sigma p)\Big) \times (t/\mathrm{BA})$$

where ΣQ^{-} is the number of cells counted in all the dissectors, h is the height of the optical dissector, a/f is the area of the counting frame, Σp is the total number of counted frames, BA is the microtome block advance to cut the block (25 μm), and t is the mean of the final section thickness (20 μm). The following formula was used to estimate the total number of bone cells: N (bone cell) = $Nv \times V$ (final) [25].

RNA extraction

Frozen bones crushed by Chinese Haven were homogenized in TRIzol (Invitrogen, USA) using a tissue laser instrument (Qiagen, GmbH). The total RNA was purified. Of the chloroform (Merck, Germany), 200 μL was added to the resultant TRIzol mixture; samples were then shaken intensely and incubated at room temperature for 5 min. Samples were centrifuged at 10,000 rpm for 20 min at 4 °C. The separated, colorless aqueous layer was mixed with 0.5 mL of isopropanol. Samples were centrifuged again at 10,000×g or 10,000 rpm for 20 min at 4 °C. The pellet was suspended in 1 mL ethanol and centrifuged at 12,000 rpm for 20 min at 4 °C. The resultant pellet was dried for 10 min at room temperature. Nuclease-free deionized water (50 μL) was added, and the RNA concentration was estimated by UV spectrophotometry at a 260-nm wavelength. Purity was assessed by ratios of A260/A280 and A260/A230.

Prior to reverse transcription, each sample was treated with RNase-free DNase I (TaKaRa Bio Inc., Japan) to remove any contaminating DNA. For RT-PCR, 1 μg total RNA was reversely transcribed to complementary DNA (cDNA) with oligo(dT) and random hexamer primers using 1 u/mL M-MLV reverse transcriptase (Invitrogen, CA, USA) at 95 °C for 15 min and 42 °C for 45 min [25].

Real-time PCR

Expression of the candidate gene development was analyzed using quantitative RT-PCR with the SYBR® Green Real-time PCR Master Mix (TaKaRa Bio, Inc.). Table 2 shows the oligonucleotide primers.

For each sample, three replicates were produced for each target gene in a final volume of 20 μL that contained 10 μL of 2× SYBR® Green PCR Master Mix, 1 μL cDNA, 2 μL of the forward and reverse primers, and 7 μL of water. Thermocycling conditions were as follows: an initial denaturation at 95 °C for 2 min, followed by 35–40 cycles of 92 °C for 15 s, 60 °C annealing for 30 s, and a 72 °C extension for 45 s. Specificity of the PCR amplification procedure was checked with a melting curve. Quantification of the relative changes in gene expression was performed using the $2^{-\Delta\Delta Ct}$ method [25]. The mRNA level of candidate genes was normalized to the signal for 18S ribosomal RNA (rRNA).

For each sample, expression was performed in a final volume of 20 μL that contained 10 μL of 2× SYBR® Green PCR Master Mix, 1 μL cDNA, 2 μL of the forward and reverse primers, and 7 μL of water. Thermocycling conditions were as follows: an initial denaturation at 95 °C for 2 min, followed by 35–40 cycles of 92 °C for 15 s, 60 °C annealing for 30 s, and a 72 °C extension for 45 s. Melting curve was used to check specificity for each PCR amplification procedure. Quantification of the relative changes in gene expression was performed using the $2^{-\Delta\Delta Ct}$ method [25]. The mRNA levels of candidate genes were normalized to the signal for 18S rRNA [25].

Statistical analysis

All data were expressed as mean ± standard errors of mean (SEMs). Normal distribution of data was analyzed using the Shapiro test. Parametric and non-parametric statistical methods were used. One-way analysis of variance (ANOVA) was used to compare changes among groups with normal distribution of data, and the least significant difference (LSD) test was used to identify differences. A p value of <0.05 was considered statistically significant. Non-parametric methods were used for statistical analysis of the other groups.

These data were analyzed using the Kruskal-Wallis and Mann-Whitney *U* tests. Difference was significant if $p < 0.005$ for analyses between groups 1 and 9. Difference was also regarded as significant if $p \leq 0.01$ for analyses between groups 1 and 5 and groups 5 and 9.

Results

General observations

Evaluations for blood glucose level and body weight of rats in the studied groups were reported in our previous study [21]. L2 weight in the studied groups are shown in Fig. 1. According to the LSD test, the vertebral weight of the DL group significantly decreased compared to DA ($p = 0.000$), DC ($p = 0.001$), DAL, and healthy (both $p = 0.003$) groups. OVX significantly decreased the vertebral weight of OA (LSD test, $p = 0.012$), OL ($p = 0.022$), and OC ($p = 0.07$) groups in comparison to the healthy group. All results are reported in Fig. 1.

Stereological analyses

Light micrographs of studied groups are shown in Fig. 2. Results of stereological analyses are shown in Figs. 3, 4, 5, 6, 7, 8, and 9.

In terms of total vertebral bone volume (mm^2), results of the LSD test demonstrated a significant decrease in total vertebral bone volume in the DL group compared to the DA ($p = 0.000$), DC and H (both $p = 0.001$), and DAL ($p = 0.003$) groups. OVX significantly decreased total vertebral bone volume of OA ($p = 0.012$), OL ($p = 0.22$), and OC ($p = 0.027$) groups compared to the healthy group. All results are shown in Fig. 3.

Results showed a significant decrease in trabecular bone volume (mm^2) in DC (LSD test, $p = 0.001$), DL ($p = 0.002$), and DAL ($p = 0.003$) compared to the healthy group. Results showed a significant decrease in trabecular bone volume of DL compared to DA ($p = 0.000$), DC ($p = 0.002$), and DAL ($p = 0.003$). There was a significant decrease in trabecular bone volume of OC, OA, OL, and OAL (all $p = 0.000$) compared to H group. All results are shown in Fig. 4.

Results showed a significant increase in cortical bone volume (mm^2) in DA (LSD test $p = 0.000$) and DC ($p = 0.001$), DAL ($p = 0.002$), and healthy ($p = 0.027$) groups compared to the DL group. A significant increase was observed in cortical bone volume in the DA group compared to H and DC groups ($p = 0.000$ and 0.007, respectively). All results are shown in Fig. 5.

Results for total bone marrow volume (mm^2) in the DL group showed significant decrease in total bone marrow volume compared to the DA (LSD test, $p = 0.000$), DAL ($p = 0.002$), and H ($p = 0.003$) groups. Significant decrease

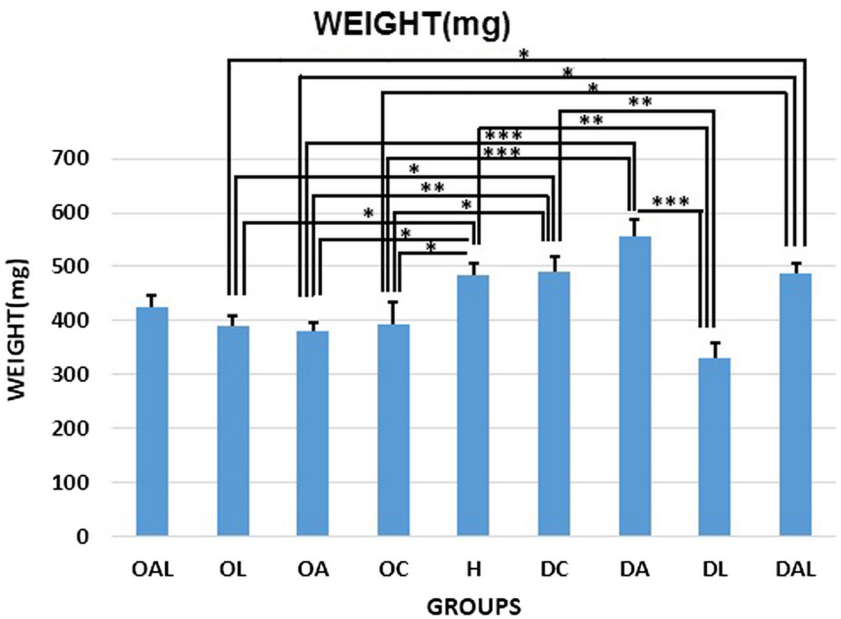

Fig. 1 Mean ± SEM of L2 vertebral weight (mg) of the studied groups compared by the LSD test; $*p < 0.05$, $**p < 0.01$, $***p < 0.001$. Ovariectomized (OVX-D) control rats (OC), OVX-D rats treated with alendronate (OA), OVX-D rats treated with laser (OL), OVX-D rats treated with laser and alendronate (OAL), healthy rats (H), dexamethasone-treated control rats (DC), dexamethasone-treated rats that received alendronate (DA), dexamethasone-treated rats that received laser (DL), and dexamethasone-treated rats that received alendronate and laser (DAL). According to the LSD test, the vertebral weight of the DL group significantly decreased compared to DA, DC, DAL, and healthy groups. OVX significantly decreased the vertebral weight of OA, OL, and OC groups in comparison to healthy group

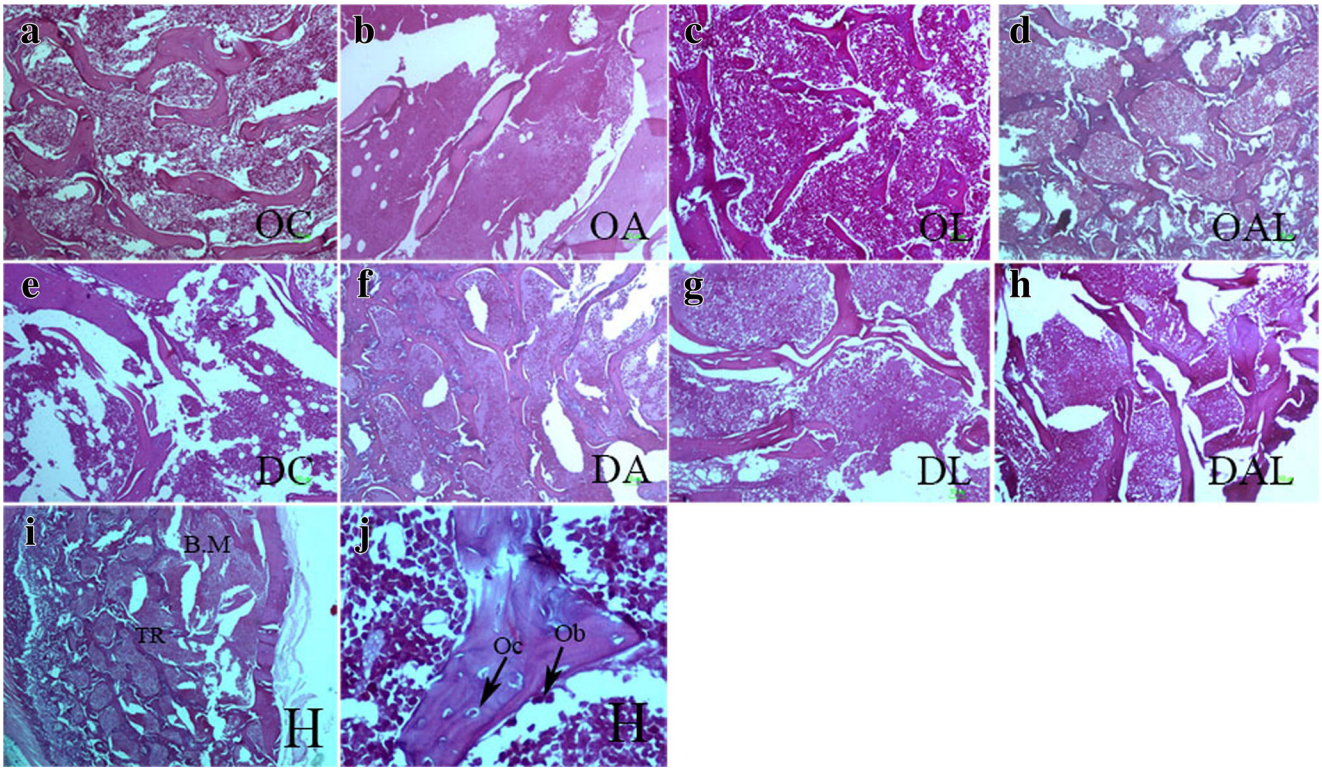

Fig. 2 Light micrographs of studied groups (H&E). *BM* bone marrow, *TR* trabecula, *oc* osteocyte, *ob* osteoblast

was observed in total bone marrow volume of OA ($p = 0.012$), OL ($p = 0.022$), and OC ($p = 0.027$) groups compared to healthy group. All results are shown in Fig. 6.

ANOVA test showed no significant differences in osteocyte numbers (10^6) of dexamethasone-treated groups. According to the LSD test, significant decreases were detected in osteocyte numbers in the OL and OC (both groups, $p = 0.000$), OA ($p = 0.005$), and OAL ($p = 0.006$) groups compared to H group. All results are shown in Fig. 7.

According to the Mann-Whitney test, there was non-significant difference in osteoblast number (10^6) in the dexamethasone-treated rats. According to the LSD test, significant decrease was recognized in osteoblast number of OC and OL groups (both $p = 0.000$) and OA ($p = 0.013$) group

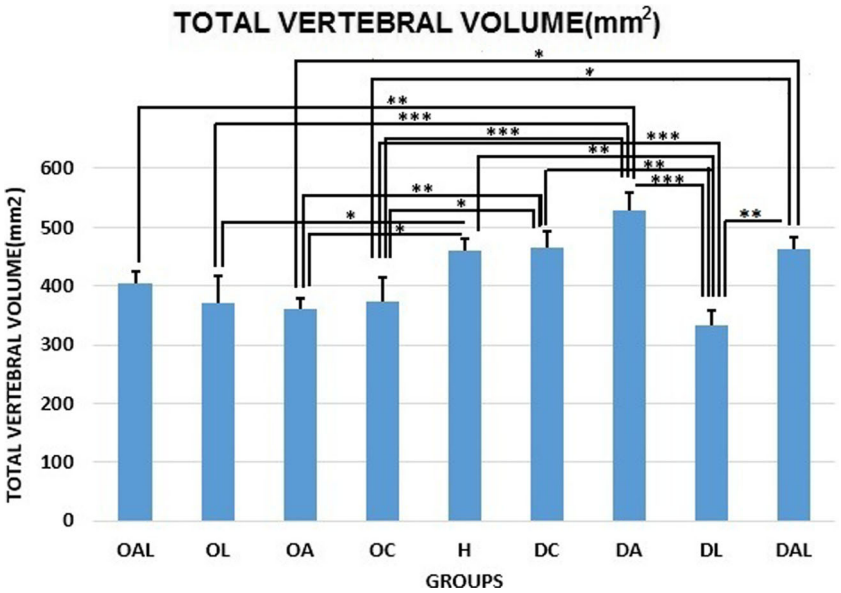

Fig. 3 Mean ± SEM of the total vertebral volume (mm^2) of the studied. Groups compared by LSD test; *$p < 0.05$, **$p < 0.01$, ***$p < 0.001$. LSD test showed a significant decrease in total vertebral bone volume in the DL group compared to DA, DC and H, and DAL groups. OVX significantly decreased total vertebral volume of OA, OL, and OC groups

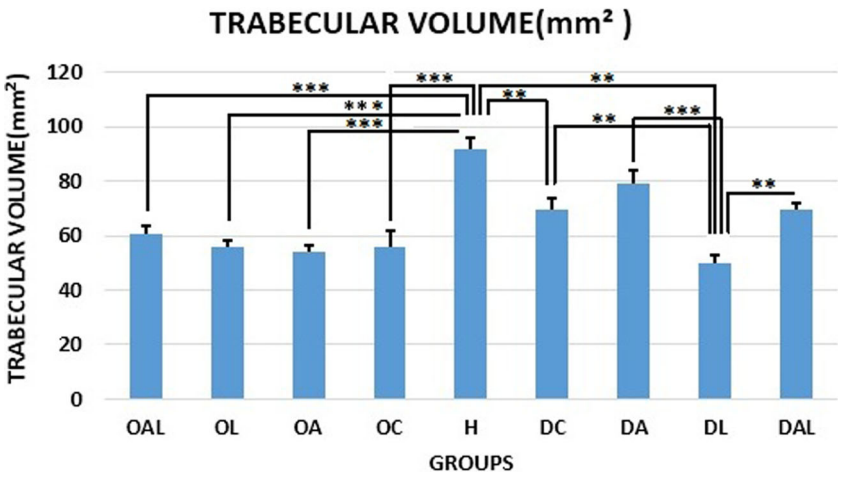

Fig. 4 Mean ± SEM of the trabecular bone volume (mm^2) of the studied groups compared by LSD test; $^{**}p < 0.01$, $^{***}p < 0.001$. There were significant differences in trabecular bone volume (mm^2) in DC, DL, and DAL compared to healthy group. We found significant decrease in trabecular bone volume of DL compared to DA, DC, and DAL. Significant decrease existed in trabecular bone volume of OC, OA, OA, and OAL compared to H group

compared to the healthy group. Significant decrease in osteoblast number of OL compared to OAL ($p = 0.005$) and OA ($p = 0.02$) as well as significant increase in osteoblast number of OA and OAL (both groups, $p = 0.003$) compared to OC. All results are shown in Fig. 8.

According to the LSD test, significant increase was discovered in osteoclast number in the DC (10^6) group compared to healthy, DAL, and DA groups (all $p = 0.000$). Significant increase existed in osteoclast number in the DL group in comparison to DAL and DA groups ($p = 0.004$ and $p = 0.005$, respectively). According to the LSD test, significant increases were determined in osteoclast number in the OC group compared to OA ($p = 0.002$), OAL ($p = 0.004$), H ($p = 0.006$), and OL ($p = 0.015$) groups. All results are shown in Fig. 9.

Real-time PCR analysis

The results of RT-PCR analysis are shown in Figs. 10, 11, 12, and 13.

According to the ANOVA test, there was non-significant difference in TGF-β1 between the studied groups. All results are demonstrated in Fig. 10.

According to the Mann-Whitney test, there was significant decrease in IGF-1 of DL group compared to DC group ($p = 0.004$). Results showed a significant decrease in IGF-1 of OL group compared to OC group ($p = 0.005$). All results are shown in Fig. 11.

According to the Mann-Whitney test, there was significant decrease in BMP-2 of DC group compared to DAL group ($p = 0.009$). Significant decrease was determined in

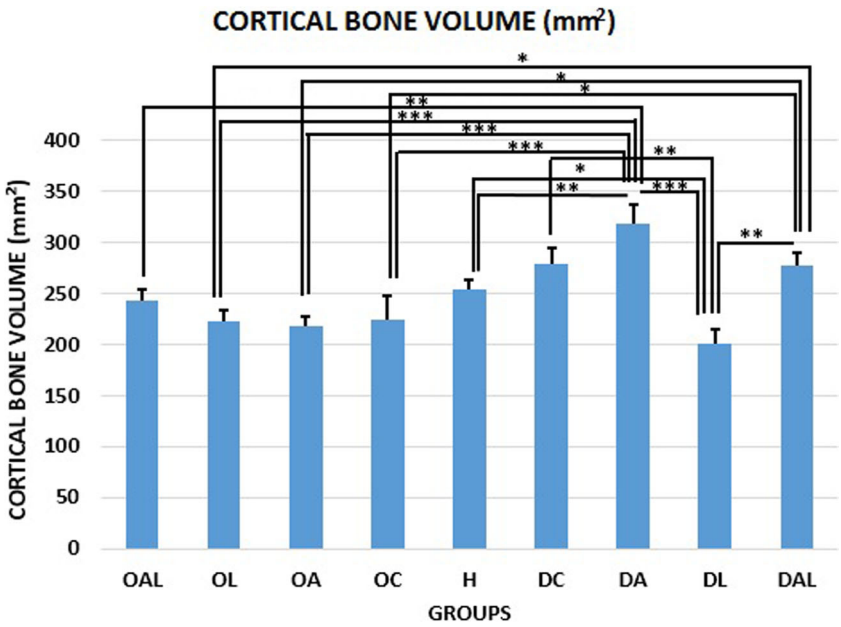

Fig. 5 Mean ± SEM of the cortical bone volume (mm^2) of the studied groups compared by LSD test; $^{*}p < 0.05$, $^{**}p < 0.01$, $^{***}p < 0.001$. There were significant increases that existed in cortical bone volume (mm^2) in DA and DC, DAL, and healthy groups compared to the DL group. We observed a significant increase in cortical bone volume in the DA group compared to the DC and H groups

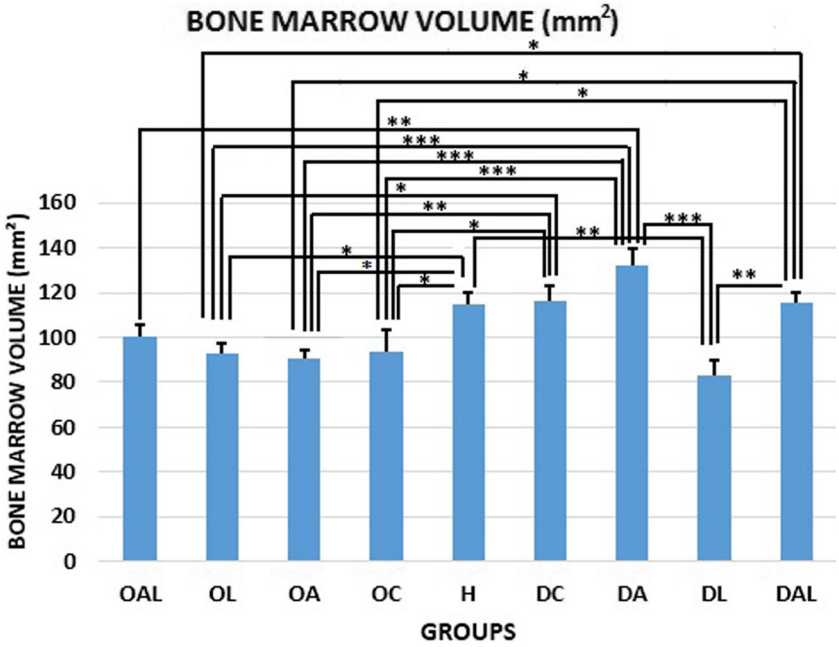

Fig. 6 Mean ± SEM of the bone marrow volume (mm^2) of the studied groups compared by LSD test; *$p < 0.05$, **$p < 0.01$, ***$p < 0.001$. DL group showed the significant decrease in total bone marrow volume compared to the DA, DAL, and H groups. We observed significant decrease in total bone marrow volume of OA and OC groups compared to healthy group. All results are shown in Fig. 5

IGF-1 of OL group compared to H and OAL groups (both $p = 0.004$). All results are shown in Fig. 12. In terms of type 1 collagen, the DL group showed significant increase compared to H and DAL groups (Mann-Whitney test $p = 0.000$ and $p = 0.004$, respectively). DA group indicated significant increase in type 1 collagen compared to H and DAL groups (Mann-Whitney test $p = 0.001$ and $p = 0.000$, respectively). And the DC group also showed significant enhancement in type 1 collagen compared to H and DAL groups (Mann-Whitney test $p = 0.004$ and $p = 0.000$, respectively). OL group showed significant increase in type 1 collagen compared to OAL and H groups (Mann-Whitney test $p = 0.004$ and $p = 0.008$, respectively). OA group indicated significant increase in type 1 collagen compared to H group (Mann-Whitney test $p = 0.008$). OC group showed significant decrease in type 1 collagen compared to H group (Mann-Whitney test $p = 0.002$). All results are illustrated in Fig. 13.

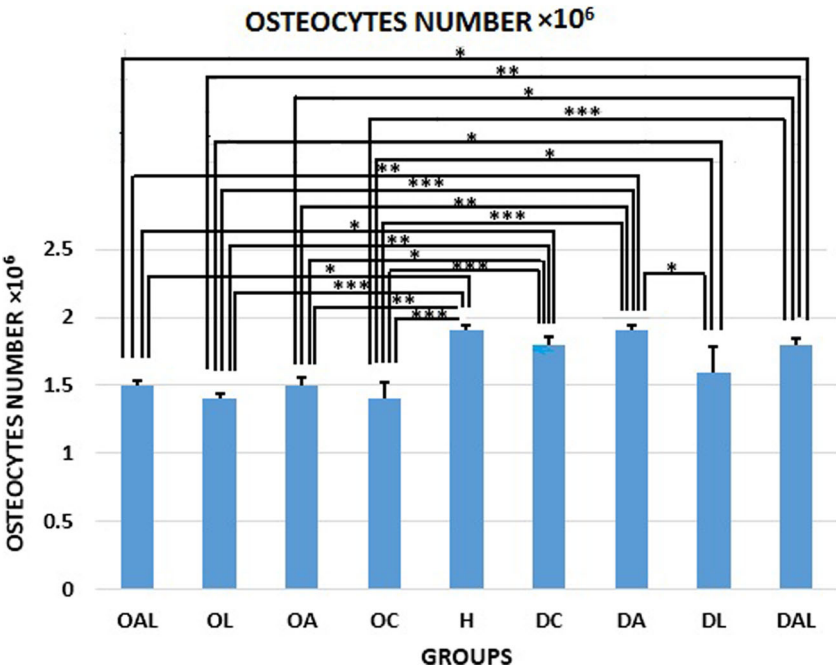

Fig. 7 Mean ± SEM of the osteocyte numbers (10^6) of the studied groups compared by ANOVA test; *$p < 0.05$, **$p < 0.01$, ***$p < 0.001$. ANOVA test showed no significant differences in osteocyte numbers (10^6) of dexamethasone-treated groups. According to the LSD test, there were significant differences in osteocyte numbers in the OL and OC, OA, and OAL groups compared to H group

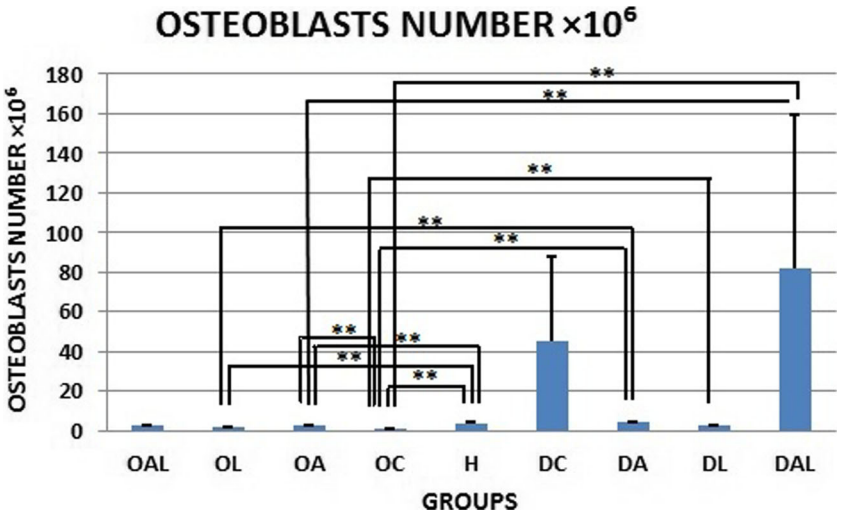

Fig. 8 Mean ± SEM of the osteoblast numbers (10^6) of the studied groups; $^{**}p < 0.01$, $^{***}p < 0.001$. Mann-Whitney test showed that there were no significant differences in osteoblast numbers (10^6) in the dexamethasone-treated rats. According to the LSD test, we observed significant decreases in osteoblast numbers of OC and OL groups, and OA group compared to healthy group. We observed significant decrease in osteoblast numbers of OL compared to OAL and OA .We also found significant increase in osteoblast numbers of OA and OAL compared to OC

Discussion

Results of the current study demonstrate that OVX-D significantly decreased evaluations of vertebral weight, total vertebral bone volume, trabecular bone volume, total bone marrow volume, osteocyte number, osteoblast number, and type 1 collagen gene expression in comparison to test results in the healthy group. Results for GIOP showed a significant decline in trabecular bone volume compared to the healthy group. Results also showed a significant increase of osteoclast number of groups of OVX-D and glucocorticoid administration compared to the healthy group. Additionally, the detrimental effect of the OVX-D procedure on bone was more serious than that of glucocorticoid administration. Furthermore, results indicated decreased trabecular bone volume in both tested models. Rapid bone loss has been reported during the first few years after menopause, especially in the trabecular compartment that results in trabecular perforation followed by entire loss of trabeculae [33]. Nordin et al. suggested that the main determinant of age-related bone loss in women was increased bone resorption and that further trabecular bone loss associated with

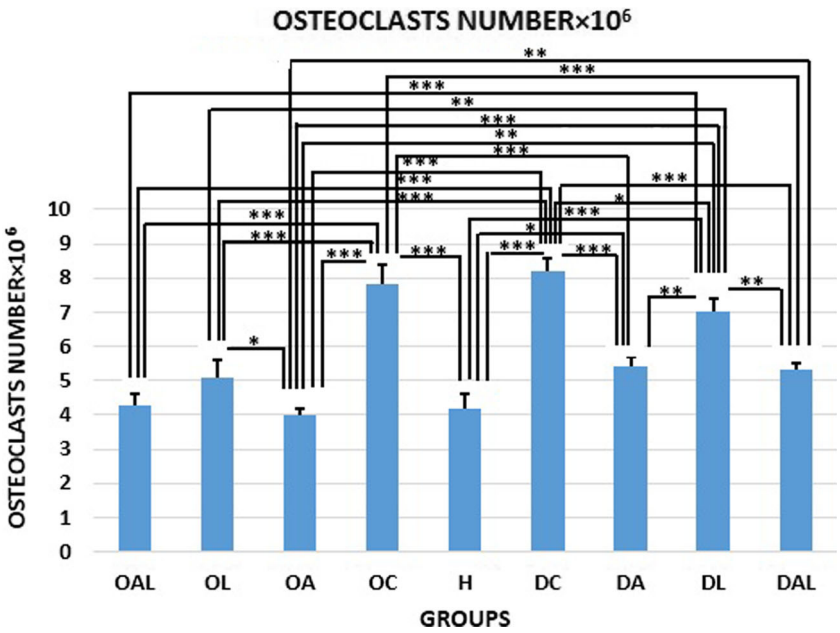

Fig. 9 Mean ± SEM of the osteoclast numbers (10^6) of the studied groups compared by LSD test; $^{*}p < 0.05$, $^{**}p < 0.01$, $^{***}p < 0.001$. There were significant increases in osteoclast numbers in the DC (10^6) group compared to healthy, DAL, and DA groups. Significant increase existed in osteoclast numbers in the DL group compared to DAL and DA groups. According to the LSD test, we observed significant increases in osteoclast numbers in the OC group compared to OA, OAL, H, and OL groups

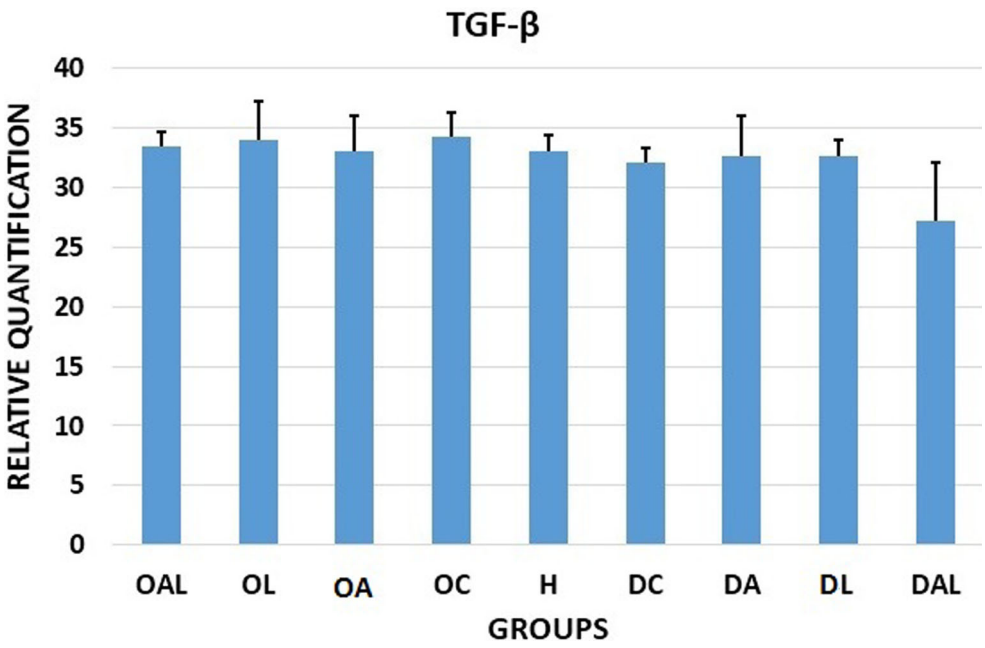

Fig. 10 Mean ± SEM of the TGF-β of the studied groups compared by ANOVA test. There were not significant differences in TGF-β between studied groups

vertebral compression was mainly attributable to a further increase in resorption [34]. In post-menopausal osteoporotic women, there is increased bone turnover [35]; the similarity to OP in OVX-D rats is associated with increased turnover due to increased resorption that exceeds bone formation [36]. This is closely associated to the direct effect of estrogen on calcium absorption that has a direct influence on bone turnover [37]. Moreover, a significant decrease of total vertebral bone volume and trabecular bone volume was determined in the OVX-D group, and a decrease of trabecular bone volume in GIOP group compared to that in healthy rats. Approximately 80% of the total skeleton are composed of cortical bone, and the rest is composed of trabecular bone. Certain regions of the skeleton are rich in trabecular bone. These areas include vertebrae, femoral neck, and distal radius [38]. There is rapid loss of trabecular bone after menopause [39]. It has been reported that GC changes the trabecular property of bone. Reports have also shown increased trabecular surface remodeling and trabecular bone structure deterioration [39, 40].

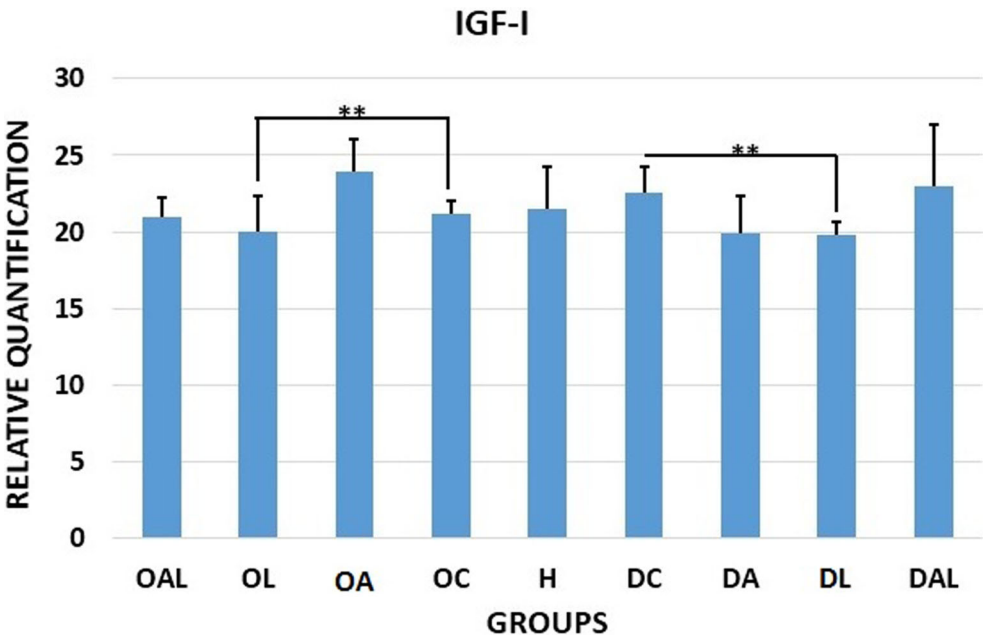

Fig. 11 Mean ± SEM of the IGF-1 of the studied groups compared by Mann-Whitney test; *$p < 0.05$, **$p < 0.01$, ***$p < 0.001$. There were significant decrease in IGF-1 of DL group compared to DC group. We also found significant decrease in IGF-1 of OL group compared to OC group

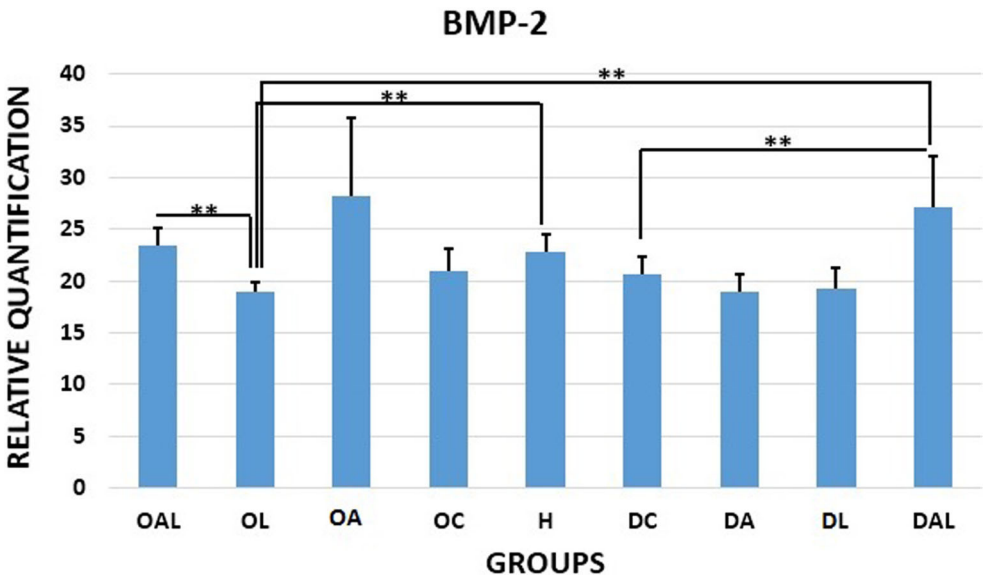

Fig. 12 Mean ± SEM of the BMP-2 of the studied groups compared by Mann-Whitney test; $^{**}p < 0.01$. According to the Mann-Whitney test, there was significant decrease in BMP-2 of DC group compared to DAL group. We found significant decrease in IGF-1 of OL group compared to H and OAL groups

Micro-architecture refers to the microscopic morphology and organization of trabecular and cortical bone. It is characterized using bone histomorphometry and micro-CT (μ-CT) scanning to obtain two-dimensional/three-dimensional measurement of the architecture at various resolutions. Estimation of the three-dimensional properties of the architecture from a two-dimensional histological section is known as stereology [41]. Stereology is typically used to determine bone micro-architecture by quantifying cortical porosity, cortical thickness, trabecular number, trabecular thickness, and trabecular connectivity; it has been illustrated that at the onset of post-menopausal OP, trabecular weakening, deeper resorption cavities, microfracture, and loss of trabecular connectivity occur [42]. Until recently, it was believed that bone loss occurred at the same extent throughout the trabecular architecture and that such loss was irreversible [7]. However, recent imaging generated by high-resolution in vivo μ-CT scanners

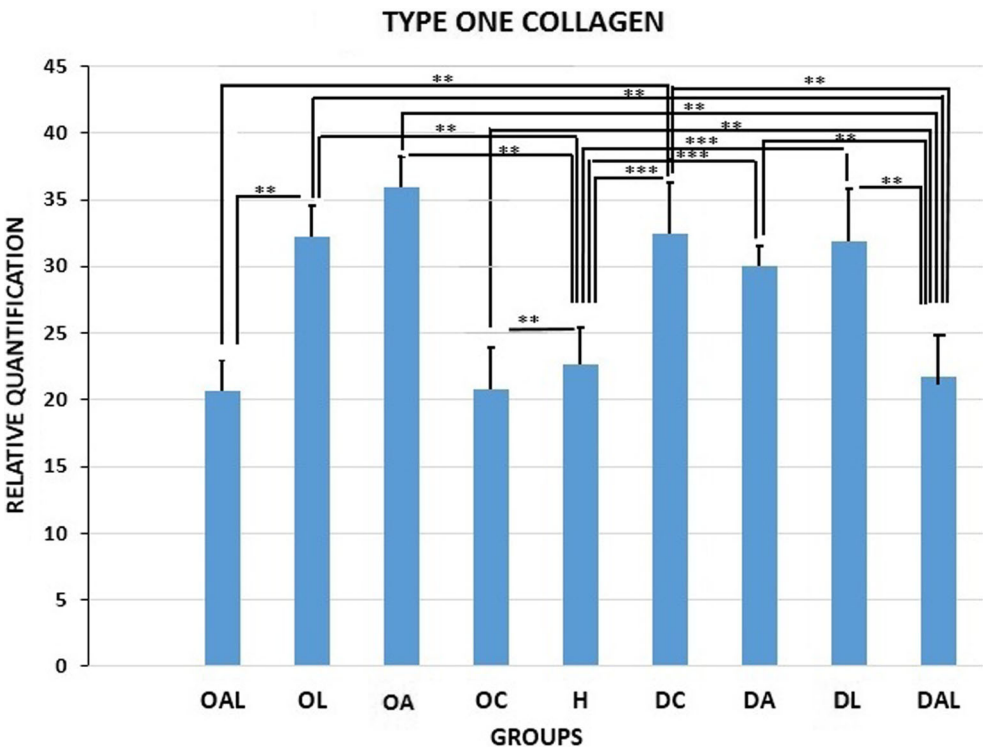

Fig. 13 Mean ± SEM of the type 1 collagen of the studied groups compared by Mann-Whitney test; $^{**}p < 0.01$, $^{***}p < 0.001$. In terms of type 1 collagen, DL group showed significant increase compared to H and DAL groups. DA group showed significant increase in type 1 collagen compared to H and DAL groups too. And also DC group showed significant increase in type 1 collagen compared to H and DAL groups too (Mann-Whitney test $p = 0.004$ and $p = 0.000$, respectively). In terms of type 1 collagen, OL group showed significant increase compared to OAL and H groups. OA group showed significant increase in type 1 collagen compared to H group. OC group showed significant decrease in type 1 collagen compared to H group

has produced new findings that question this assumption. Waarsing et al. report that following initial trabecular thinning in OVX-D rats, the few remaining trabecular subsequently recovered slowly and increased in thickness [43, 44]. Stereological results showed that laser significantly decreased total vertebral bone volume, trabecular bone volume, cortical bone volume, and bone marrow volume in glucocorticoid-treated rats compared to those in the healthy group; laser also significantly decreased total vertebral bone volume, bone marrow volume, osteocyte number, and osteoblast number in OVX-D rats.

Bone is a complex tissue. Its fundamental function is to resist mechanical injury and absorb pressure. Bone strength depends on quantity of bone tissue and its quality, which is outlined by the geometry and shape of the bone, the micro-architecture of the trabecular bone morphology, cortical thickness, and porosity; it is also characterized by intrinsic properties of bony tissue such as turnover, mineral, and collagen. These determinants of bone quality are interrelated, especially mineral and collagen, and analysis of their specific roles in bone strength is difficult to identify. The major complication of some bone diseases such as osteoporosis, i.e., fracture, is due to weak bone strength. Therefore, any treatment of OP relies on improving bone strength. Bone strength is indirectly measured by BMD using dual-energy X-ray absorptiometry (DXA). Since DXA-measured BMD represents 60–70% of the variation in bone strength, some important factors are not determined by DXA, in terms of the effects of antiosteoporotic treatment and the progression of OP. In addition to BMD, geometry and trabecular micro-architecture also need consideration. Thus, evaluation of the intrinsic mechanical quality of bone should provide a better understanding of the role of tissue quality in determining bone strength [38, 45, 46]. Consistent with results of our recent study, it is reported that laser significantly improved important biomechanical parameters of the vertebrae in glucocorticoid-induced OP and OVX-D tests compared to results of healthy and control groups, respectively [21].

Osteoblast cells synthesize collagen during the initial phase of bone formation when unmineralized bone (osteoid) is made. The collagen molecules are assembled extracellularly and immature ketomine and aldimine cross-links are formed; these contribute to the formation of mature pyridinium or pyrrole cross-links. Together, these cross-links result in fibril formation that act as a scaffold for bone minerals and provide strength [7, 46, 47]. The collagen in bone is primarily type I collagen, but types III, IV, and VI are also present [48]. At the onset of post-menopausal OP, diverse changes in the compositional properties of the collagen have been reported; a recent study indicates that synthesis of type I collagen enhanced during OP, while earlier studies reported reduced amounts of type VI collagen and type III collagen [7, 49].

It was determined that evaluations of vertebral weight, total vertebral bone volume, trabecular bone volume, cortical bone volume, and total bone marrow volume of the DA group were significantly higher in comparison to results from the DL group and that number of osteoclasts in the DA group was significantly lower than that of the DL group ($p = 0.005$). It was also found that osteoblast number of the OA group was significantly higher compared to the OL group.

Bisphosphonates are currently used as a first-line therapeutic agent for OP. Bisphosphonates inhibit bone resorption by selective adsorption to a mineral surface and subsequent internalization by bone-resorbing osteoclasts where they interfere with various biochemical processes. Alendronate inhibits a key enzyme, farnesyl pyrophosphate synthase, in the mevalonate pathway that prevents biosynthesis of isoprenoid compounds that are considered essential for post-translational modification of small guanosine triphosphate (GTP)-binding proteins. Both protein prenylation and function of these regulatory proteins are impaired, leading to osteoclast dysfunction [48]. Results of the current study demonstrated that alendronate alone was statistically more effective than laser alone on the above-mentioned stereological parameters.

In the present study, the effects of laser irradiation were examined on IGF-I and BMP-2, which are considered as the most important factors in bone formation in healthy animals [49]. There is evidence to show that expression of molecules that modulate osteoblast activity may be altered during post-menopausal osteoporosis. During physiologic bone resorption, growth factors such as IGF-I and TGF-β are released from the extracellular matrix, which recruit and activate osteoblasts to begin collagen synthesis [7]. Osteogenic and adipogenic processes are modulated by the BMP-2. This cytokine regulates expression of the nuclear receptor peroxisome proliferator-activated receptor-γ (PPARγ) and Runt-related transcription factor 2 (RUNX2) [50]. Laser can promote bone formation and inhibit bone resorption, thus facilitating bone remodeling [12–15]. However, it was demonstrated that laser significantly decreased IGF-I and BMP-2 in both tested models of OP.

Interestingly, it was found that laser treated in both test models of OP showed significant increase of type 1 collagen gene expression compared to those in the healthy group. Results for laser in OVX-D rats and GIOP rats in combination showed significantly increased osteoblast number and type 1 collagen gene expression, and significantly decreased osteoclast number compared to control groups. These results (significant increase of type 1 collagen gene expression) may be in agreement with increasing biomechanical properties of the osteoporotic vertebrae in the laser-treated rats as recently reported in Bayat et al. [21]. Bayat et al. report on an evaluation of the effects of laser on cancellous bone strength in OVX-D and GIOP test model of OP. There were four OVX-D groups and four dexamethasone-treated groups. Laser (890 nm,

80 Hz, 5.5 J/cm^2) was carried out on the spinal processes of the vertebrae T12, L1, L2, and L3. Biomechanical test findings indicate a positive influence of laser and alendronate administration on increasing bending stiffness and maximum force of the osteoporotic bones in comparison to the healthy group. Furthermore, laser treatment of OVX-D rats significantly escalated stress high load compared to OVX-D control rats. Bayat et al. concluded that laser conserved cancellous (trabecular) bone of vertebrae against the detrimental influence of OVX-D osteoporosis on bone strength in rats in comparison to the control.

These results demonstrate that laser alone had a detrimental effect on many stereological parameters such as total vertebral bone volume, trabecular bone volume, cortical bone volume, and bone marrow volume in both glucocorticoid-treated rats and OVX-D rats compared to those in the healthy group. Furthermore, results showed that the combination of alendronate and laser in OVX-D rats and GIOP rats significantly increased osteoblast number and type 1 collagen gene expression and significantly decreased osteoclast number compared to that of the controls. The results of this study were in agreement with result of other studies. Diniz et al. report on evaluation on the effect of laser in combination with alendronate sodium on osteopenic bone. Laser (GaAlAs; 830 nm, 50 mW, and 4 J/cm^2) on the femoral neck and vertebral segments were performed. In the osteopenic + alendronate sodium group, the trabecular bone volume in L2 was significantly higher than that in the controls. Notably, in the combination between laser and alendronate sodium, the trabecular bone volume in osteoporotic animals was significantly higher in vertebrae L2 and T13 than osteoporotic bone and was similar to that in the sham-operation group. Diniz et al. demonstrated that treatment with laser together with bisphosphonate therapy was the most effective on reversing vertebral osteopenia due to the ovariectomy [28].

Mohsenifar et al. reported an investigation of the effect of laser on the cortical bone of osteoporotic rat tibia in two test models, GIOP rats and OVX-D rats. GIOP rats and OVX-D rats treated with alendronate (1 mg/kg) and laser (890 nm, 80 Hz, 0.972 J/cm^2). Rats were given alendronate for 30 days and subjected to laser three times per week for 8 weeks. Tests demonstrated a significant rise in cortical bone volume in all study groups compared to healthy rats. Results showed significant reduction in trabecular bone volume in all study groups compared to healthy rats. The control rats with OP showed significantly increased osteoclast number. Alendronate significantly decreased osteoclast number in osteoporotic rats. In the laser + alendronate group, the same effect was observed on osteoporotic bone [25]. Fridoni et al. report on the effects of laser on cortical bone in OVX-D and GIOP test models of OP in rats. The osteoporotic rats received alendronate for 30 days. Laser (890 nm, 80 Hz, 0.972 J/cm^2) was performed on the tibia three times per week for 2 months. After 2 months, tibia were extracted and submitted to a three-point bending test. Laser did not enhance the biomechanical parameters of osteoporotic bones compared to controls and healthy rats. Laser with alendronate treatment significantly increased stress high load in OVX-D rats compared to those in the healthy group [26].

The physical parameters used in PW laser such as wavelength, power (peak power, average power, and power density),pulse frequency, pulse duration (width), duration of exposure, and energy density all impact the biological effects of laser irradiation [32, 51]. PW laser at 5.5-J/cm^2 energy density and other delivery parameters used in the current study failed to cause any beneficial effects in the histological and gene expression parameters of osteoporotic bones. A probable cause is the relatively lower energy density of laser employed in this study. The applied dose was selected in accordance with two studies that demonstrated increased bone density in rats from an 890-nm infrared laser at 0.972 J/cm^2 [19, 32].

Recently, Muniz Renno et al. studied the effects of PBM (830 nm, 100 W/cm^2, 120 J/cm^2) on femurs of exercised osteoporotic rats. The exercise program and the laser radiation were performed 48 h over an 8-week period. The exercise program consisted of jumps. Femurs were submitted to a physical and geometrical property evaluation, a biomechanical test, and calcium and phosphorus evaluation. Muniz Renno et al. concluded that exercised animals showed higher bone strength and physical property values. However, the PBM did not improve the biostimulatory effects of the exercise on the osteoporotic rats [30].

It was concluded that PBM alone had a detrimental effect on many stereological parameters of vertebral bone such as total vertebral bone volume, trabecular bone volume, cortical bone volume, and bone marrow volume in both GIOP rats and OVX-D rats compared the healthy group. Alendronate significantly improved many stereological parameters such as total vertebral bone volume, trabecular bone volume, cortical bone volume, and bone marrow volume in both GIOP rats and OVX-D rats compared to those in laser groups. Furthermore, the combination of alendronate and laser in OVX-D rats and GIOP rats significantly increased osteoblast number and type 1 collagen gene expression. Since the PBM had osteogenic effects, different laser parameters should be examined to verify whether an appropriate laser protocol alone or administration with a proper antiosteoporotic agent might reverse the detrimental effects of OP. We suggest measuring Ca^{++} levels on blood in further studies.

Compliance with ethical standards

Role of funding source This article is financially supported by "the Research Department" at Shahid Beheshti University of Medical Sciences, Tehran, Iran (Grant No. 10397-1391-1-115-1092).

Conflict of interest The authors declare that they have no conflict of interest.

Ethical approval The procedure was approved by the Medical Ethics Committee of Shahid Beheshti University of Medical Sciences, Tehran, Iran (protocol no. 1391-1-115-1092).

Informed consent This study was performed on animal model, so it was not included of "Informed Consent."

References

1. Bidwell JP, Alvarez MB, Hood M Jr, Childress P (2013) Functional impairment of bone formation in the pathogenesis of osteoporosis: the bone marrow regenerative competence. Curr Osteoporos Rep 1: 117–125. doi:10.1007/s11914-013-0139-2
2. Briot K, Roux C (2015) Glucocorticoid-induced osteoporosis. RMD Open 1:e000014. doi:10.1136/rmdopen-2014-000014
3. Bouillon R, Burckhardt P, Christiansen C, Fleisch H, Fujita T, Gennari C et al (1991) Consensus development conference: prophylaxis and treatment of osteoporosis. Am J Med 90:107–110
4. Wright NC, Looker AC, Saag KG, Curtis JR, Delzell ES, Randall S et al (2014) The recent prevalence of osteoporosis and low bone mass in the United States based on bone mineral density at the femoral neck or lumbar spine. J Bone Miner Res 29:2520–2526. doi:10.1002/jbmr.2269
5. Mansjur KQ, Kuroda S, Izawa T, Maeda Y, Sato M, Watanabe K, et al (2016) The effectiveness of human parathyroid hormone and low-intensity pulsed ultrasound on the fracture healing in osteoporotic bones. Ann Biomed Eng 1–9. doi:10.1007/s10439-015-1533-y
6. Izzah Ibrahim N, Mohamad S, Mohamed N, Nazrun SA (2013) Experimental fracture protocols in assessments of potential agents for osteoporotic fracture healing using rodent models. Curr Drug Targets 14:1642–1650. doi:10.2174/13894501146661312162240003
7. McNamara L (2010) Perspective on post-menopausal osteoporosis: establishing an interdisciplinary understanding of the sequence of events from the molecular level to whole bone fractures. J R Soc Interface 7:353–372. doi:10.1098/rsif.2009.0282
8. Khosla S, Westendorf JJ, Oursler MJ (2008) Building bone to reverse osteoporosis and repair fractures. J Clin Invest 118:421–428. doi:10.1172/JCI33612
9. Cashman KD (2007) Diet, nutrition, and bone health. J Nutr 137: 2507S–2512S
10. Tee S-I, Yosipovitch G, Chan YC, Chua SH, Koh ET, Chan YH, Tan SS, Tsou IY, Tan SH (2012) Prevention of glucocorticoid-induced osteoporosis in immunobullous diseases with alendronate: a randomized, double-blind, placebo-controlled study. Arch Dermatol 148:307–314. doi:10.1001/archdermatol.2011.354
11. da Silva JP, da Silva MA, Almeida APF, Junior IL, Matos AP (2010) Laser therapy in the tissue repair process: a literature review. Photomed Laser Surg 28:17–21. doi:10.1089/pho.2008.2372
12. Ueda Y, Shimizu N (2003) Effects of pulse frequency of low-level laser therapy (LLLT) on bone nodule formation in rat calvarial cells. J Clin Laser Med Surg 21:271–277. doi:10.1089/104454703322564479
13. Ueda Y, Shimizu N (2001) Pulse irradiation of low-power laser stimulates bone nodule formation. J Oral Sci 43:55–60. doi:10.2334/josnusd.43.55
14. Sohn H, Ko Y, Park M, Kim D, Moon YL, Jeong YJ, Lee H, Moon Y, Jeong BC, Kim O, Lim W (2015) Effects of light-emitting diode irradiation on RANKL-induced osteoclastogenesis. Lasers Surg Med 47:745–755. doi:10.1002/lsm.22413
15. Kiyosaki T, Mitsui N, Suzuki N, Shimizu N (2010) Low-level laser therapy stimulates mineralization via increased Runx2 expression and ERK phosphorylation in osteoblasts. Photomed Laser Surg 28(Suppl 1):S167–S172. doi:10.1089/pho.2009.2693
16. Xu M, Deng T, Mo F, Deng B, Lam W, Deng P, Zhang X, Liu S (2009) Low-intensity pulsed laser irradiation affects RANKL and OPG mRNA expression in rat calvarial cells. Photomed Laser Surg 27:309–315. doi:10.1089/pho.2008.2283
17. Bayat M, Abdi S, Javadieh F, Mohsenifar Z, Rashid MR (2009) The effects of low-level laser therapy on bone in diabetic and nondiabetic rats. Photomed Laser Surg 27:703–708. doi:10.1089/pho.2008.2351
18. Freidouni M, Nejati H, Salimi M, Bayat M, Amini A, Noruzian M, Asgharie MA, Rezaian M (2015) Evaluating glucocorticoid administration on biomechanical properties of rats' tibial diaphysis. Iran Red Crescent Med J 17(3):e19389. doi:10.5812/ircmj.19389 eCollection 2015
19. Najar A, Fridoni M, Rezaei F, Bayat S, Bayat M (2015) Supraphysiologic glucocorticoid administration increased biomechanical bone strength of rats' vertebral body. Lab Anim Res 31: 180–187. doi:10.5625/lar.2015.31.4.180
20. Cressoni MD, Giusti HH, Piao AC, de Paiva Carvalho RL, Anaruma CA, Casarotto RA (2010) Effect of GaAlAs laser irradiation on the epiphyseal cartilage of rats. Photomed Laser Surg 28: 527–532. doi:10.1089/pho.2009.2572
21. Bayat M, Fridoni M, Nejati H, Mostafavinia A, Salimi M, Ghatrehsamani M et al (2016) An evaluation of the effect of pulsed wave low-level laser therapy on the biomechanical properties of the vertebral body in two experimental osteoporosis rat models. Lasers Med Sci 31:305-14. doi:10.1007/s10103-015-1842-2
22. Ko CY, Kang H, Ryu Y, Jung B, Kim H, Jeong D, Shin HI, Lim D, Kim HS (2013) The effects of minimally invasive laser needle system on suppression of trabecular bone loss induced by skeletal unloading. Lasers Med Sci 28:1495–1502. doi:10.1007/s10103-013-
23. Kang H, Ko CY, Ryu Y, Seo DH, Kim HS, Jung B (2012) Development of a minimally invasive laser needle system: effects on cortical bone of osteoporotic mice. Lasers Med Sci 27:965–969. doi:10.1007/s10103-011-1014-y
24. Chen Y, Cao Z, Zhang L, Xu X, Chen Y, Chen Y (2011) Low level laser can be a novel adjuvant method for orthodontic tooth movement on postmenopausal women. Med Hypotheses 76:479–481. doi:10.1016/j.mehy.2010.11.025
25. Mohsenifar Z, Fridoni M, Ghatrehsamani M, Abdollahifar MA, Abbaszadeh H, Mostafavinia A, Fallahnezhad S, Asghari M, Bayat S, Bayat M (2016) Evaluation of the effects of pulsed wave LLLT on tibial diaphysis in two rat models of experimental osteoporosis, as examined by stereological and real-time PCR gene expression analyses. Lasers Med Sci 31:721–732. doi:10.1007/s10103-016-1916-9
26. Fridoni M, Masteri Farahani R, Nejati H, Salimi M, Gharavi SM, Bayat M, Amini A, Torkman G, Bayat S (2015) Evaluation of the effects of LLLT on biomechanical properties of tibial diaphysis in two rat models of experimental osteoporosis by a three point bending test. Lasers Med Sci 30:1117–1125. doi:10.1007/s10103-014-1706-1
27. Medalha CC, Amorim BO, Ferreira JM, Oliveira P, Pereira RM, Tim C, Lirani-Galvão AP, da Silva OL, Renno AC (2010) Comparison of the effects of electrical field stimulation and low-level laser therapy on bone loss in spinal cord-injured rats. Photomed Laser Surg 28:669–674. doi:10.1089/pho.2009.2691
28. Diniz JS, Nicolau RA, de Melo ON, do Carmo Magalhães F, de Oliveira Pereira RD, Serakides R (2009) Effect of low-power gallium-aluminum-arsenium laser therapy (830 nm) in combination with bisphosphonate treatment on osteopenic bone structure: an experimental animal study. Lasers Med Sci 24:347–352. doi:10.1007/s10103-008-0568-9
29. Renno AC, de Moura FM, dos Santos NS, Tirico RP, Bossini PS, Parizotto NA (2006) Effects of 830-nm laser light on preventing

bone loss after ovariectomy. Photomed Laser Surg 24:642–645. doi:10.1089/pho.2006.24.642
30. Muniz Renno AC, de Moura FM, dos Santos NS, Tirico RP, Bossini PS, Parizotto NA (2006) The effects of infrared-830 nm laser on exercised osteopenic rats. Lasers Med Sci 21:202–207. doi:10.1007/s10103-006-0396-8
31. Kanis J, McCloskey E, Johansson H, Cooper C, Rizzoli R, Reginster J-Y (2013) European guidance for the diagnosis and management of osteoporosis in postmenopausal women. Osteoporos Int 24:23–57. doi:10.1007/s00198-012-2074-y
32. Hashmi JT, Huang YY, Sharma SK, Kurup DB, De Taboada L, Carroll JD, Hamblin MR (2010) Effect of pulsing in low-level light therapy. Lasers Surg Med 42:450–466. doi:10.1002/lsm.20950
33. Je A, Nb M, Sagreiya K (1987) The microanatomy of trabecular bone loss in normal aging men and women. Clin Orthop Relat Res 215:260–271 **3802645**
34. Nordin B, Speed R, Aaron J, Crilly R (1981) Bone formation and resorption as the determinants of trabecular bone volume in postmenopausal osteoporosis. Lancet 318:277–279 6114324
35. Van Brussel M, Bultink I, Lems W (2009) Prevention of glucocorticoid-induced osteoporosis. Expert Opin Drug Deliv 10: 997–1005. doi:10.1517/14656560902868225
36. Yeh J, Chen M-M, Aloia J (1996) Ovariectomy-induced high turnover in cortical bone is dependent on pituitary hormone in rats. Bone 18:443–450
37. Jagtap VR, Ganu JV, Nagane NS (2011) BMD and serum intact osteocalcin in postmenopausal osteoporosis women. Indian J Clin Biochem 26:70–73
38. Green D, Wallace H (2003) Late effects of childhood cancer. CRC Press
39. Parfitt AM (1987) Trabecular bone architecture in the pathogenesis and prevention of fracture. Am J Med 82:68–72
40. Lane NE, Yao W, Balooch M, Nalla RK, Balooch G, Habelitz S et al (2006) Glucocorticoid-treated mice have localized changes in trabecular bone material properties and osteocyte lacunar size that are not observed in placebo-treated or estrogen-deficient mice. J Bone Miner Res 21:466–476. doi:10.1359/JBMR.051103
41. Russ JC, Dehoff RT (2012) Practical stereology. Springer Science & Business Media
42. Lane NE, Thompson JM, Haupt D, Kimmel DB, Modin G, Kinney JH (1998) Acute changes in trabecular bone connectivity and osteoclast activity in the ovariectomized rat in vivo. J Bone Miner Res 13:229–236. doi:10.1359/jbmr
43. Waarsing J, Day J, Van der Linden J, Ederveen A, Spanjers C, De Clerck N, Sasov A, Verhaar JA, Weinans H (2004) Detecting and tracking local changes in the tibiae of individual rats: a novel method to analyse longitudinal in vivo micro-CT data. Bone 34:163–169
44. Waarsing JH, Day JS, Verhaar JA, Ederveen AG, Weinans H (2006) Bone loss dynamics result in trabecular alignment in aging and ovariectomized rats. J Orthop Res 24:926–935. doi:10.1002/jor.20063
45. Ammann P (2002) Determining factors of bone mechanical resistance. Therapie 58:403–407. doi:10.2515/Therapie:2003065
46. Viguet-Carrin S, Garnero P, Delmas P (2006) The role of collagen in bone strength. Osteoporos Int 17:319–336. doi:10.1007/s00198-005-2035-9
47. Eyre DR, Dickson I, Van Ness K (1988) Collagen cross-linking in human bone and articular cartilage. Age-related changes in the content of mature hydroxypyridinium residues. Biochem J 252:495–500
48. Bailey A, Wotton S, Sims T, Thompson P (1993) Biochemical changes in the collagen of human osteoporotic bone matrix. Connect Tissue Res 29:119–132
49. Fujimoto K, Kiyosaki T, Mitsui N, Mayahara K, Omasa S, Suzuki N, Shimizu N (2010) Low-intensity laser irradiation stimulates mineralization via increased BMPs in MC3T3-E1 cells. Lasers Surg Med 42:519–526. doi:10.1002/lsm.20880/full
50. Donoso O, Pino AM, Seitz G, Osses N, Rodríguez JP (2015) Osteoporosis-associated alteration in the signaling status of BMP-2 in human MSCs under adipogenic conditions. J Cell Biochem 116:1267–1277. doi:10.1002/jcb.25082
51. Bayat M (2014) The necessity for increased attention to pulsed low-level laser therapy. Photomed Laser Surg 32(8):427–428. doi:10.1089/pho.2014.9858